FINITE TEMPERATURE MOTT TRANSITION IN A NONLOCAL PNJL MODEL*

Sanjin Benić

Physics Department, Faculty of Science, University of Zagreb, Zagreb, Croatia

David Blaschke

Institute of Theoretical Physics, University of Wrocław, Wrocław, Poland
Bogoliubov Laboratory for Theoretical Physics, JINR Dubna, Dubna, Russia
Fakultät für Physik, Universität Bielefeld, Bielefeld, Germany

(Received July 3, 2013)

We provide a novel calculation of the Mott effect in nonlocal PNJL models. We find that the "deconfinement" transition temperature in these models is lower than the Mott temperature. Furthermore, the mass and the width of the σ and the π meson modes is calculated with the result that the width in nonlocal models is, in general, reduced as compared to local models. Difficulties encountered while attempting to "Wick rotate" covariant models are carefully discussed.

DOI:10.5506/APhysPolBSupp.6.947
PACS numbers: 11.10.St, 05.70.Jk, 12.39.Ki, 11.30.Rd

1. Introduction

It is by now established that the first rise in the QCD pressure, as calculated from the lattice, is well described by the Hadron Resonance Gas [1, 2]. This important result offers a simple physical picture in understanding a phase transition from the hadronic world to the quark-gluon plasma: with an increase of the temperature, the meson wave functions start to overlap. Due to Pauli blocking, quarks are then forced to occupy higher quantum "states" and finally merge into the continuum, see Fig. 1. Moreover, it calls for a description of the lattice data within a unified field-theoretical model, where the meson degrees of freedom are interpreted as true $\bar{q}q$ bound states. Such a microscopic description might be vital for understanding the quark–hadron transition in general [3, 4].

* Presented at the Workshop "Excited QCD 2013", Bjelašnica Mountain, Sarajevo, Bosnia–Herzegovina, February 3–9, 2013.

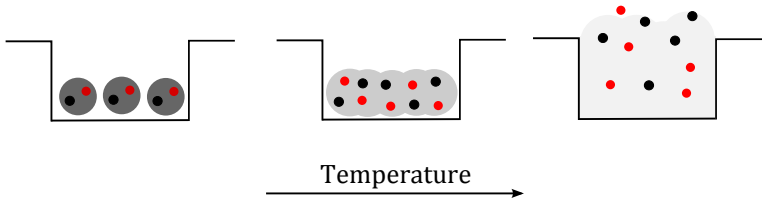

Fig. 1. (Color online) An illustration of the Mott transition. The bound states represented by shaded area are shown in a schematic potential well. Color brightness accounts for the strength of the interaction.

In this contribution, we provide a brief explorative account of this *Mott transition* in a covariant, nonlocal, Polyakov–Nambu–Jona-Lasinio (nl-PNJL) model [5–8]. Quark models, in general, have a potential to offer a powerful theoretical setup for a systematic introduction of fluctuations beyond the mean field, leading to a virial expansion-type description of QCD thermodynamics. Important progress in that direction has been achieved recently [6, 9–11].

2. Selected features of the model

The nl-PNJL models are characterized by the running of the mass function in the quark propagator provided by $M(p^2) = m + \sigma f(p^2)$. In order to properly address the Mott transition, it is important to study the analytic properties of the quark propagator. The latter is highly non-trivial due to the fact that the mass "runs" in a covariant fashion. Utilizing a Gaussian form factor $f(p^2) = e^{-p^2/\Lambda^2}$, it is easy to show that the propagator exhibits an infinite sequence of complex conjugate mass poles (CCMPs), if the gap σ is above the critical value $\sigma_{\rm c} = \Lambda/\sqrt{2e}$. For $\sigma < \sigma_{\rm c}$, the complex pole, together with its complex conjugate counterpart "fuses" into a doublet of real poles $zz^* \to HL$, as shown in Fig. 2. In the chiral limit ($m = 0$), real poles are provided by the Lambert W-function

$$m^2_{L,H}(\sigma) = -\tfrac{1}{2} W_{0,-1}\left(-2\sigma^2/\Lambda^2\right) , \tag{1}$$

where the "heavy" state is non-physical in the sense of $m_H \to \infty$ as $\sigma \to 0$. By contrast, the "light" state quickly joins the mass gap σ at high T, where it can be interpreted as a physical state, see Fig. 2.

For the model parameters which we employ here [12], always holds $\sigma > \sigma_{\rm c}$. Therefore, the physical continuum of states appears only at temperatures above $T > T_{\rm cont}$.

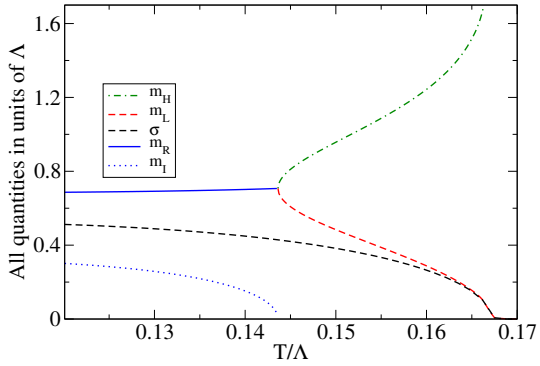

Fig. 2. (Color online) Temperature dependence of the lowest lying CCMPs in the chiral limit and without the Polyakov loop. The imaginary part of the singularity vanishes when the temperature rises to the point where $\sigma(T_{\rm cont}) = \sigma_{\rm c} = \Lambda/\sqrt{2e}$.

3. Finite temperature π and σ correlations

The central object of our study is the meson polarization function [13–16]

$$\Pi_M(\nu_m, |\boldsymbol{q}|) = \frac{d_q}{3} T \sum_n \int \frac{d^3p}{(2\pi)^3} \mathrm{tr}_C \left[f^2(p_n^2) \frac{K_M\left(\omega_n^2, \boldsymbol{p}^2, \nu_m^2, \boldsymbol{q}^2\right)}{\mathcal{D}((p_n^-)^2)\mathcal{D}((p_n^+)^2)} \right], \quad (2)$$

with $d_q = 2 \times 2 \times N_f \times N_c$ being the quark degrees of freedom, and

$$K_M\left(\omega_n^2, \boldsymbol{p}^2, \nu_m^2, \boldsymbol{q}^2\right) = (p_n^+ p_n^-) \pm M\left((p_n^+)^2\right) M\left((p_n^-)^2\right). \quad (3)$$

We use the following notation: $M = \pi, \sigma$, $q_m = (\nu_m, \boldsymbol{q})$, where $\nu_m = 2m\pi T$ are the bosonic Matsubara frequencies. Furthermore, $p_n^{\pm} = (\omega_n^{\pm}, \boldsymbol{p}^{\pm})$, with $\omega_n^{\pm} = \omega_n \pm \nu_m/2$ and $\boldsymbol{p}^{\pm} = \boldsymbol{p} \pm \boldsymbol{q}/2$, and

$$\mathcal{D}\left(-z^2, \boldsymbol{p}^2\right) = -z^2 + \boldsymbol{p}^2 + M^2\left(-z^2 + \boldsymbol{p}^2\right). \quad (4)$$

3.1. Imaginary part of the polarization function

In a first attempt to discuss the Mott effect, we consider the meson masses as given by the spatial, or screening masses, from the respective Bethe–Salpeter equations $1 - G_S \Pi_M(\nu_m = 0, |\boldsymbol{q}| = -im_M) = 0$, while for the widths we calculate the imaginary part of (2). Details of this calculation

are provided in [17]. For the meson at rest $\boldsymbol{q} = 0$, we find

$$\mathrm{Im}[\Pi_M(-iq_0,0)] = \frac{d_q}{16\pi}\left[1-2n_\Phi(q_0/2)\right]\sqrt{1-\left(\frac{2m_L}{q_0}\right)^2} f^2\left(\frac{q_0^2}{4}-m_L^2\right) \times \frac{K_M\left(0,\frac{q_0^2}{4}-m_L^2,-q_0^2,0\right)}{\left[\mathcal{D}'\left(-\frac{q_0^2}{4},\frac{q_0^2}{4}-m_L^2\right)\right]^2}\,\theta\left(\frac{q_0}{2}-m_L\right), \tag{5}$$

where $n_\Phi(z)$ is the generalized occupation number function in the presence of the Polyakov loop Φ. For details, see *e.g.* Ref. [18]. In the local limit $f \to 1$, it is easy to show that the standard PNJL result [18] is correctly reproduced. In deriving this formula, we have ignored the threshold for the meson to decay to a heavy state $M \to HH$, as well as possible mixed channels $H \to ML$. For the meson width, we use

$$\Gamma_M = g_{M\bar{q}q}\frac{\mathrm{Im}[\Pi_M]}{m_M}, \tag{6}$$

where $g_{M\bar{q}q}$ is the residue of the meson propagator. In numerical calculations, we assume that the leading effect of $g_{M\bar{q}q}$ is to cancel the f^2 term in $\mathrm{Im}[\Pi_M]$.

4. Results and conclusion

In Fig. 3 we present results of our approach. Besides the spatial meson masses and widths, the "continuum" states defined by $2m_{qp}$, where $m_{qp} = m+\sigma$, are also shown. Strictly speaking, these states are not present as real

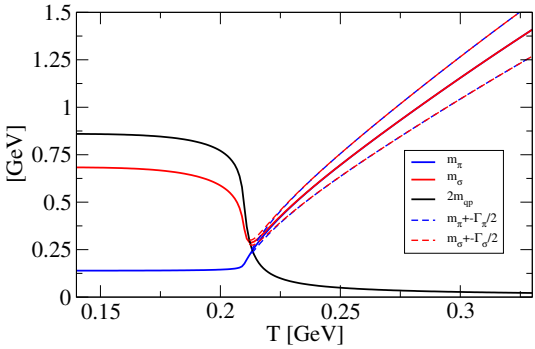

Fig. 3. (Color online) Masses of π (light gray/blue) and σ meson (dark gray/red). The "continuum" threshold $2m_{\mathrm{qp}}$ is shown in black. The range of a half-width around the meson mass is given by dashed lines.

singularities of the quark propagator up to $T_{\rm cont}$, giving a distinctive feature of covariant models. Nevertheless, at $T > T_{\rm cont}$, they are almost identical to the actual singularities, see Fig. 2 and, therefore, provide an intuitive picture also in the low temperature region.

As the temperature increases, the continuum threshold drops, eventually hitting the meson masses at the Mott temperature $T_{\rm Mott}$. From that point on, the sharp meson states become resonances by acquiring a finite width. Around the same temperature the σ and the π meson become degenerate thus making the restoration of the chiral symmetry manifest.

In contrast to the local PNJL calculation, see *e.g.* [18], we find a smaller width, and a significantly higher mass, their ratio being even around $\Gamma_M/M_M \sim 0.1$ at $T \sim 300$ MeV, see Fig. 3. The latter is a common feature of spatial masses.

While the presented calculation already reveals some aspects of the nonlocality of the interaction, namely a significant reduction of the width of the resonance, the crucial step in properly accounting for the Mott transition in covariant models is still lacking. While at low T we expect bound states to dominate the thermodynamics, the 2-particle correlation contribution in the high temperature regime shall come from the quark–antiquark scattering [9–11].

We find that in covariant models such an approach is hindered by the additional (unphysical) singularities, making the original physical picture blurry. For example, to account for the scattering, one needs to put quarks on shell (which is possible after $T_{\rm cont}$). This calls for a Wick rotation of the effective interaction itself. At least with a Gaussian regulator such an approach would yield a term $e^{q_0^2/\Lambda^2}$, where q_0 is the typical energy of the process. Thus, when $q_0 \sim T \sim \Lambda$, scattering would seemingly grow without bound and eventually violate unitarity.

It is then clear that knowing the effective dressing of the quarks only in Euclidean space is insufficient. Moreover, one easily imagines that by using different analytic choices for the regulators in Euclidean space, these might behave quite differently in the complex energy plane, although being qualitatively the same in Euclidean space. We believe that a more appropriate "gauge" for fully accounting the physics of the Mott transition might be the Coulomb gauge [19–21], or its covariant formulations [22], where the interaction does not depend on the energy.

REFERENCES

[1] F. Karsch, K. Redlich, A. Tawfik, *Phys. Lett.* **B571**, 67 (2003).

[2] S. Borsanyi *et al.*, *J. High Energy Phys.* **1009**, 073 (2010).

[3] D. Blaschke, F. Reinholz, G. Röpke, D. Kremp, *Phys. Lett.* **B151**, 439 (1985).

[4] L. Turko, D. Blaschke, D. Prorok, J. Berdermann, arXiv:1307.1732 [nucl-th].

[5] D. Horvatic, D. Blaschke, D. Klabucar, O. Kaczmarek, *Phys. Rev.* **D84**, 016005 (2011).

[6] A.E. Radzhabov, D. Blaschke, M. Buballa, M.K. Volkov, *Phys. Rev.* **D83**, 116004 (2011).

[7] T. Hell, K. Kashiwa, W. Weise, *Phys. Rev.* **D83**, 114008 (2011).

[8] J.P. Carlomagno, D.G. Dumm, N.N. Scoccola, arXiv:1305.2969 [hep-ph].

[9] A. Wergieluk, D. Blaschke, Y.L. Kalinovsky, A. Friesen, arXiv:1212.5245 [nucl-th].

[10] K. Yamazaki, T. Matsui, arXiv:1212.6165 [hep-ph].

[11] D. Blaschke, D. Zablocki, M. Buballa, G. Roepke, arXiv:1305.3907 [hep-ph].

[12] D. Gomez Dumm, A.G. Grunfeld, N.N. Scoccola, *Phys. Rev.* **D74**, 054026 (2006).

[13] D. Blaschke *et al.*, *Int. J. Mod. Phys.* **A16**, 2267 (2001).

[14] A. Scarpettini, D. Gomez Dumm, N.N. Scoccola, *Phys. Rev.* **D69**, 114018 (2004).

[15] D. Horvatic, D. Blaschke, D. Klabucar, A.E. Radzhabov, *Phys. Part. Nucl.* **39**, 1033 (2008).

[16] G.A. Contrera, D.G. Dumm, N.N. Scoccola, *Phys. Rev.* **D81**, 054005 (2010).

[17] S. Benic, D. Blaschke, G.A. Contrera, D. Horvatic, arXiv:1306.0588 [hep-ph].

[18] H. Hansen *et al.*, *Phys. Rev.* **D75**, 065004 (2007).

[19] P. Guo, A.P. Szczepaniak, *Phys. Rev.* **D79**, 116006 (2009).

[20] M. Pak, H. Reinhardt, *Phys. Lett.* **B707**, 566 (2012).

[21] P. Watson, H. Reinhardt, *Phys. Rev.* **D86**, 125030 (2012).

[22] V.G. Morozov, G. Röpke, A. Höll, *Theor. Math. Phys.* **131**, 812 (2002).